

Instability mechanisms in a low-Mach-number reacting flow from coupled convection-reaction-diffusion equations

V. V. Pulikkottil and R. I. Sujith

Citation: *Physics of Fluids* **27**, 074101 (2015); doi: 10.1063/1.4923233

View online: <http://dx.doi.org/10.1063/1.4923233>

View Table of Contents: <http://scitation.aip.org/content/aip/journal/pof2/27/7?ver=pdfcov>

Published by the [AIP Publishing](#)

Articles you may be interested in

[Absolute and convective instabilities of heated coaxial jet flow](#)

Phys. Fluids **27**, 054101 (2015); 10.1063/1.4919594

[Coupling between hydrodynamics, acoustics, and heat release in a self-excited unstable combustor](#)

Phys. Fluids **27**, 045102 (2015); 10.1063/1.4916673

[Flow noise induced by small gaps in low-Mach-number turbulent boundary layers](#)

Phys. Fluids **25**, 110821 (2013); 10.1063/1.4823830

[Absolute and convective instabilities of an inviscid compressible mixing layer: Theory and applications](#)

Phys. Fluids **21**, 104101 (2009); 10.1063/1.3225142

[Dispersion relations for the convective instability of an acidity front in Hele-Shaw cells](#)

J. Chem. Phys. **121**, 935 (2004); 10.1063/1.1760515

Did your publisher get
18 MILLION DOWNLOADS in 2014?
AIP Publishing did.



THERE'S POWER IN NUMBERS. Reach the world with AIP Publishing.



Instability mechanisms in a low-Mach-number reacting flow from coupled convection-reaction-diffusion equations

V. V. Pulikkottil^{a)} and R. I. Sujith

*Department of Aerospace Engineering, Indian Institute of Technology Madras,
Chennai, TN 600036, India*

(Received 15 January 2015; accepted 16 June 2015; published online 2 July 2015)

In this paper, instability mechanisms in a low Mach number reacting flow are investigated. Here, the emphasis is on the growth or decay of acoustic oscillations which arise from the acoustic-hydrodynamic interaction in a low Mach number reacting flow. Motivated by the studies in magnetohydrodynamics and atmospheric flows, we propose to investigate the acoustic-hydrodynamic coupling as a system of wave-mean flow interaction. For example, a comparison with the heat fluctuation modified hydrodynamics associated with magnetohydrodynamics is useful in understanding this coupling. The wavelike acoustic disturbance is introduced here as a compressibility correction to the mean flow. Accounting for the multiple scales introduced by the weak compressibility, we derive a set of equations governing wave-mean flow interaction in a reacting low Mach number flow. Sources such as volume expansion (which, in atmospheric flows arises due to the density variation with altitude) occur in reacting flows due to the heat release rate. This heat release rate, when coupled with the acoustic field, often leads to self-sustained thermo-acoustic oscillations. In the study of such oscillations, we discover a relation between the acoustic pressure and second order thermal fluctuations. Further, using this relation, we discover the nonlinear coupling mechanism that would lead to self-sustained oscillations in a reacting low Mach number flow. This mechanism, represented by a coupled convection reaction diffusion system, is presented here for the first time. In addition to the acoustic pressure and temperature fields, we also discover the role of acoustic velocity field in the acoustic-hydrodynamic interaction through a convective and lift-up mechanism. © 2015 AIP Publishing LLC. [<http://dx.doi.org/10.1063/1.4923233>]

I. INTRODUCTION

In a reacting low Mach number flow, an acoustic field introduces weak compressibility in an otherwise incompressible flow. Zank and Matthaeus¹ described such a flow as nearly incompressible fluid flow. In magnetohydrodynamic (MHD) flows, Zank and Matthaeus¹ studied the effect of weak compressibility using the method of multiple scales (MMS). Such an approach is not unique to the study of MHD. In atmospheric flows, where density varies with altitude, a similar system has been studied.² Accounting for density inhomogeneity, Bühler² derived a system of equations for describing wave-mean flow interaction. This system of equations resembles that of nearly incompressible fluid flow derived by Zank and Matthaeus.¹ Following Zank and Matthaeus,¹ Hunana *et al.*³ extended the analysis to include large scale density inhomogeneity in the solar wind. The description of wave-mean flow interaction in atmospheric flows and nearly incompressible flows in MHD resembles that of a reacting low Mach number flow.

Mechanisms responsible for wave-mean flow interaction vary from one system to another. In a nearly incompressible fluid flow as found in MHD, there is a mutual coupling between the magnetohydrodynamic turbulence and the acoustic field.⁴ The volume expansion due to the density inhomogeneity influences the waves in atmospheric flows.² In a reacting flow, volume expansion

^{a)}Electronic mail: vinuvargheseijk@gmail.com

is one of the sources driving the acoustic field. Here, the volume expansion is due to the heat release rate from chemical reaction. This volume expansion can become unsteady when it occurs in response to the unsteady heat release rate. We will show in this paper that such a process can lead to the nonlinear evolution of acoustic field variables. In reacting flows, when the acoustic driving is stronger than the damping in the system, the acoustic-hydrodynamic interaction can establish a positive feedback loop, leading to self-sustained acoustic oscillations.⁵ This phenomenon is known as “thermo-acoustic instability.” Thermo-acoustic oscillation is a consequence of acoustic-hydrodynamic interaction in reacting flows.⁵⁻⁷

These self-sustained acoustic oscillations introduce localized fluctuations in the heat release rate. Apart from that, vortex shedding⁵ or parametric instability of flame⁸ also result in localized heat release rate fluctuations. The spatial scale corresponding to these fluctuations is much shorter compared to the long wavelength acoustic wave. We will derive equations to describe the influence of the heat release rate fluctuations on the wave-mean flow interaction.

Towards this purpose, we need to know the mechanisms responsible for heat release rate modification in a reacting low Mach number flow. Dunlap⁹ suggested a possibility where the reaction rate is modified by the second order thermal fluctuations or acoustic pressure fluctuations. Consistent with the earlier theoretical studies,¹⁰⁻¹² we will use the terms “temperature coupling” and “pressure coupling” to describe such processes.

In addition, Markstein¹³ suggested a velocity coupling mechanism in which the heat release rate is modified by the gas flow velocity around the flame. The modified heat release rate, in turn, modifies the gas flow velocity. Based on the equations derived for acoustic-hydrodynamic interaction, we show that the above mentioned coupling mechanisms due to gas flow velocity, acoustic pressure, and thermal fluctuations are essentially nonlinear. We show that this nonlinear behavior contributes to the self-sustained oscillations in a thermo-acoustic system.

Theoretical studies on these nonlinear mechanisms focus on the rate of growth or decay of acoustic oscillations.^{10-12,14} These studies necessitate a characteristic time scale for describing the growth or decay of acoustic oscillations. The necessity for two time scales, an acoustic time scale and a characteristic time scale for the growth or decay of acoustic amplitude, is thus clear from the earlier theoretical studies.^{10-12,15} Later in this paper, based on these earlier studies, we will determine a characteristic time scale that describes the coupling process responsible for the growth or decay of acoustic oscillations.

The coupling mechanisms have their origin in the acoustic-hydrodynamic interaction. Analytical studies for acoustic-hydrodynamic interaction are limited to cases where the reaction zone is compact (length scale of the reaction zone is much less than the acoustic wavelength) and can be treated as a discontinuity.¹⁴⁻¹⁶ A Rankine-Hugoniot relation is used to relate the acoustic velocity across the discontinuity.^{14,15} However, in such cases, the acoustic pressure does not vary across the reaction zone.¹² Matalon and Matkowsky¹⁶ and Wu *et al.*^{14,15} showed that when the flame is treated as discontinuity, the acoustic-hydrodynamic interaction is governed by the velocity coupling. For a distributed mean heat release rate, such as in a well stirred reactor, the flame can no longer be treated as a discontinuity and the acoustic pressure varies across the flame. For such a case, Clavin *et al.*^{10,11} suggest the existence of pressure and temperature coupling.

These coupling mechanisms are essentially related to the heat release rate from chemical reaction. Therefore, the first step towards understanding pressure, temperature, and velocity couplings is to find out how the fluctuations of pressure, temperature, and velocity lead to the heat release rate fluctuation.¹⁰ While deriving the governing equations for acoustic-hydrodynamic interaction, we will show that finding such a relation is possible once we understand the order of magnitudes of fluctuations in pressure, velocity, and temperature due to the acoustic field. Clavin *et al.*¹⁰ provide us with such an understanding, where they suggest the order of fluctuations with respect to the mean flow variables.

A subsequent study by Clavin *et al.*¹¹ shows the influence of the order of magnitude of acoustic pressure and acoustic velocity on the heat release rate fluctuation. With this insight, and considering the fluctuation of heat release due to turbulence, they modeled a nonlinear acoustic pressure equation to study the transition of thermo-acoustic system to instability or self-sustained oscillations. They investigated the nonlinear evolution of the acoustic pressure caused by turbulence. The

nonlinear effects, arising from the coupling between the hydrodynamic field and the acoustic field, were examined earlier by Culick^{17,18} for compressible flows. He describes a “gas dynamic nonlinearity” due to the acoustic source terms $u' \cdot \nabla u'$ and $p' \nabla p'$, where u' and p' are the acoustic velocity and pressure, respectively. However, in the case of weak compressibility, as in the case of nearly incompressible flow, contribution from such terms is negligible when compared to the nonlinear terms due to heat release rate.

This weak compressibility, however, gives rise to self-sustained acoustic oscillations. Our objective is to reveal the fundamental mechanisms of acoustic-hydrodynamic interaction leading to such oscillations. An investigation in that direction will lead to a general theory for instability in low Mach number reacting flows. An understanding of the nonlinear processes introduced by weak compressibility, when extended to include density inhomogeneity and volume expansion due to heat release rate, helps to explain the origin of self-sustained oscillations in low Mach number flows.

In this paper, from the equations governing compressible fluid flow, we will derive equations describing the acoustic-hydrodynamic interaction. Using these equations, we will derive a nonlinear equation describing the growth or decay of acoustic oscillations. Physical mechanisms such as pressure coupling, temperature coupling, and velocity coupling will be explained using the equations for acoustic-hydrodynamic interaction. We show the significance of these coupling mechanisms in the origin of self-sustained oscillations, by deriving nonlinear coupled convection reaction diffusion (CRD) equations. Our CRD equations, which show the influence of heat release rate fluctuations in determining the nonlinear evolution of acoustic pressure, are introduced for the first time to study the stability of reacting low Mach number flows. For demonstrating the influence of heat release rate on the self-sustained oscillations, we have used a reaction-diffusion (RD) system, by neglecting the effect of convection in CRD equations, to predict the transition to self-sustained acoustic pressure oscillation. Then, we solve the full convection reaction diffusion system to study the change in the nature of transition due to convective effects. We will also prove, by describing the nonlinear evolution of acoustic pressure amplitude as a function of convective time scale, the role of convective time scale as the characteristic time scale for describing the acoustic-hydrodynamic interaction.

II. DERIVATION OF NONLINEAR EQUATIONS FROM COMPRESSIBLE FLUID FLOW EQUATIONS

A. Governing equations

The governing equations, nondimensionalized by their reference variables, are given as follows:¹⁹

$$\frac{\partial \rho}{\partial t} + \nabla \cdot (\rho \vec{u}) = 0, \quad (1)$$

$$\frac{\partial \rho u}{\partial t} + \nabla \cdot (\rho \vec{u} \vec{u}) + \frac{1}{\gamma M^2} \nabla p = \frac{1}{Re} \nabla \cdot \tau, \quad (2)$$

$$\frac{1}{(\gamma - 1)} \frac{Dp}{Dt} = - \frac{\gamma}{(\gamma - 1)} p \nabla \cdot \vec{u} + H Da \dot{Q} + \frac{1}{RePr} \nabla^2 T, \quad (3)$$

$$\frac{\partial \rho Y_i}{\partial t} + \nabla \cdot \rho Y_i \vec{u} = \frac{1}{ReSc} \nabla^2 Y_i + Da \omega_k. \quad (4)$$

Equations (1)-(4) are the continuity, momentum, energy, and species conservation equations, respectively, for compressible flow. Here, ρ , p , and T are density, pressure, and temperature, respectively, and \vec{u} is the velocity vector. The reaction rate ω_k follows the Arrhenius rate law. In Eq. (3), Da , H , and \dot{Q} are the Damkohler number, heat release parameter, and heat release rate, respectively.

B. Method of multiple scales

The next step is to construct a solution expansion for the field variables. Towards this purpose, we follow earlier theoretical studies.¹⁰⁻¹² Clavin *et al.*¹⁰ and Pelce and Rochwerger¹² have suggested

orders of magnitude for the acoustic field variables in the context of combustion instability. Clavin *et al.*¹⁰ suggest that the acoustic pressure and temperature perturbations to be of the same order. The acoustic velocity perturbation is $O(1/M)$ times the acoustic pressure perturbation. Based on the order of magnitudes, the acoustic perturbation variables are ordered as follows:

$$\rho = \rho_0 + \epsilon^2 \rho_2, \quad (5)$$

$$\vec{u} = \vec{u}_0 + \epsilon \vec{u}_1, \quad (6)$$

$$p = p_0 + \epsilon^2(p_{2h} + p_{2a}), \quad (7)$$

$$T = T_0 + \epsilon^2 T_2. \quad (8)$$

To eliminate the singular coefficient $1/(\gamma M^2)$ of the pressure gradient term in Eq. (2), the hydrodynamic pressure variable p_{2h} is chosen to be of second order (ϵ^2) in solution expansion (7).¹⁹ The small number ϵ is proportional to the Mach number ($\epsilon = \sqrt{\gamma}M$). The heat release rate expansion is determined based on the suggestion by Clavin *et al.*,¹⁰ following which, the mean heat release rate \dot{Q}_0 is expressed to be of the same order as the heat release rate fluctuation (due to the acoustic wave) \dot{Q}' ,

$$\dot{Q} = \dot{Q}_0 + \dot{Q}'. \quad (9)$$

All the hydrodynamic field variables are written with subscript 0, except p_{2h} which is written at a higher order to eliminate the singular term with coefficient $1/(\gamma M^2)$. In Eqs. (5)-(8), p_{2h} and p_{2a} are the hydrodynamic pressure and acoustic pressure, respectively. The acoustic velocity is written as \vec{u}_1 . The higher order variable ρ_2 represents the acoustic density fluctuation. T_2 represents the second order thermal fluctuation. The mean heat release rate along with its fluctuations due to hydrodynamics is represented with \dot{Q}_0 . The heat release rate fluctuation due to acoustic wave is represented at the same order of the mean heat release rate as \dot{Q}' .

The low Mach number limit introduces two time scales and two length scales as $\tau = \tau'/\epsilon$ and $\eta = \xi/\epsilon$, where τ and τ' are the acoustic and the convective time scales, respectively. The spatial scales η and ξ are the hydrodynamic and long wavelength acoustic length scales, respectively. The operator splitting is performed as $\partial/\partial t = (1/\epsilon)\partial/\partial \tau + \partial/\partial \tau'$ for the temporal operator and $\nabla = \epsilon\nabla_\xi + \partial\nabla_\eta$ for the spatial operator.¹ The equations governing the hydrodynamics are obtained at leading order in ϵ as follows:

$$\frac{\partial \rho_0}{\partial \tau'} + \nabla_\eta \cdot \rho_0 \vec{u}_0 = 0, \quad (10)$$

$$\frac{\partial \rho_0 \vec{u}_0}{\partial \tau'} + \nabla_\eta \cdot (\rho_0 \vec{u}_0 \vec{u}_0) + \nabla_\eta p_{2h} - \frac{1}{Re} \nabla_\eta \cdot \tau_0 = 0, \quad (11)$$

$$\frac{1}{(\gamma - 1)} \frac{\partial p_0}{\partial \tau'} = \frac{-\gamma}{(\gamma - 1)} [\rho_0 \nabla_\eta \cdot \vec{u}_0] \quad (12)$$

$$+ HDa(\dot{Q}_0 + \dot{Q}') + \frac{1}{RePr} \nabla_\eta^2 T_0,$$

$$\frac{\partial \rho_0 Y_{i0}}{\partial \tau'} + \nabla_\eta \cdot \rho_0 Y_{i0} \vec{u}_0 = \frac{1}{ReSc} \nabla_\eta^2 Y_{i0} + Da\omega_k, \quad (13)$$

$$p_0 = \rho_0 T_0. \quad (14)$$

Equations (10)-(13) imply that the short length scale η and the convective time scale τ' govern the unsteady hydrodynamics and the resulting unsteady heat release rate.

The fast time scale equation for \vec{u}_1 is obtained from the leading order momentum equation following Zank and Matthaeus,¹

$$\frac{\partial \rho_0 \vec{u}_1}{\partial \tau} + \nabla_\eta p_{2a} = 0. \quad (15)$$

The density perturbation equation at $O(\epsilon)$ is as follows:

$$\frac{\partial \rho_2}{\partial \tau} + \nabla_\eta \cdot (\rho_0 \vec{u}_1) + \nabla_\xi \cdot (\rho_0 \vec{u}_0) = 0. \quad (16)$$

Equation (16) has derivatives in two length scales. An equation on the long length scale may provide an unbounded solution ($\nabla_\xi = 1/\epsilon \nabla_\eta$) as $\epsilon \rightarrow 0$. This is the consequence of non-zero divergence $\nabla \cdot \vec{u}_0$. The non-zero divergence or the dilatation term is the consequence of the heat release rate during combustion. Later in this paper, the dilatation term will be shown as a source term for the acoustic pressure. Averaging the fluctuations over the short length scale, the evolution equation for ρ_2 in the acoustic time scale is obtained,

$$\frac{\partial \overline{\rho_2}}{\partial \tau} = -\nabla_\xi \cdot \overline{\rho_0 \vec{u}_0}. \quad (17)$$

Integration yields

$$\rho_2 = \tau [-\nabla_\xi \cdot \overline{\rho_0 \vec{u}_0}]. \quad (18)$$

Since the hydrodynamic variables ρ_0 , u_0 , and T_0 are independent of the acoustic time scale, $\rho_2 \rightarrow \infty$ as $\epsilon \rightarrow 0$ which is the case since $\tau = \tau'/\epsilon$. To ensure the convergence of the solution expansion, we have to impose a solvability condition²⁰ as $\nabla_\xi \cdot \rho_0 \vec{u}_0 = 0$. In other words, we have eliminated the dependence of the hydrodynamic variables on the long length scale. The resulting acoustic time scale equation for the density perturbation ρ_2 is

$$\frac{\partial \rho_2}{\partial \tau} + \nabla_\eta \cdot (\rho_0 \vec{u}_1) = 0. \quad (19)$$

At $O(\epsilon)$, the acoustic time scale equation for acoustic pressure perturbation is obtained as

$$\begin{aligned} \frac{\partial p_{2a}}{\partial \tau} + \gamma p_0 \nabla_\eta \vec{u}_1 &= -\gamma p_0 \nabla_\xi u_0 \\ &+ \frac{\gamma}{RePr} [\nabla_\eta \nabla_\xi T_0 + \nabla_\xi \nabla_\eta T_0]. \end{aligned} \quad (20)$$

Integration with respect to τ will lead to the following expression for p_{2a} :

$$\begin{aligned} p_{2a} &= \tau [-\gamma p_0 \nabla_\xi u_0 + \frac{\gamma}{RePr} [\nabla_\eta \nabla_\xi T_0 \\ &+ \nabla_\xi \nabla_\eta T_0]] - \gamma p_0 \int \nabla_\eta \vec{u}_1 + C(t, \eta, \xi). \end{aligned} \quad (21)$$

The acoustic perturbation velocity \vec{u}_1 is a function of acoustic time scale τ . The terms with coefficient τ will grow linearly as $\epsilon \rightarrow 0$. We have imposed the solvability condition

$$-\gamma p_0 \nabla_\xi u_0 + \frac{\gamma}{RePr} [\nabla_\eta \nabla_\xi T_0 + \nabla_\xi \nabla_\eta T_0] = 0 \quad (22)$$

to ensure the convergence of the solution expansion for pressure variable ($p = p_0 + \epsilon^2(p_{2h} + p_{2a})$). The equation for acoustic perturbation pressure p_{2a} on the acoustic time scale is obtained as

$$\frac{\partial p_{2a}}{\partial \tau} + \gamma p_0 \nabla_\eta \vec{u}_1 = 0. \quad (23)$$

From Eqs. (15) and (23), the linear wave equations for \vec{u}_1 and p_{2a} are obtained as

$$\frac{\partial^2 p_{2a}}{\partial \tau^2} - \nabla_\eta \cdot c_0^2 \nabla_\eta p_{2a} = 0, \quad (24)$$

$$\frac{\partial^2 \vec{u}_1}{\partial \tau^2} - c_0^2 \nabla_\eta^2 \vec{u}_1 = 0, \quad (25)$$

where c_0 is the speed of sound. Here, we will assume a solution of the form $A_i(\eta, \xi, \tau') e^{i\omega\tau}$ for the perturbation variables, where $A_i = (\hat{\rho}_2, \hat{\vec{u}}_1, \hat{p}_{2a}, \hat{T}_2)$ and $e^{i\omega\tau}$ is the part of the solution which satisfies Eqs. (24) and (25). These equations imply that whenever there is a non-zero amplitude A_i , the acoustic pressure and velocity field variables admit an oscillatory solution.

The momentum equation at $O(\epsilon)$, the continuity equation at $O(\epsilon^2)$, and the energy equation at $O(\epsilon^2)$ yield the convective time scale equations for \vec{u}_1 , ρ_2 , and p_{2a} . The solution form $A_i(\eta, \xi, \tau') e^{i\omega\tau}$ is substituted in the equations for \vec{u}_1 , ρ_2 , and p_{2a} . Applying the conditions for solvability and collecting terms with coefficient $e^{i\omega\tau}$, a set of weakly nonlinear equations are obtained

for the convective time scale,

$$\frac{\partial \hat{u}_1}{\partial \tau'} + \frac{1}{\rho_0} \nabla_\xi \hat{p}_{2a} = -\vec{u}_0 \cdot \nabla_\eta \hat{u}_1 - \hat{u}_1 \cdot \nabla_\eta \vec{u}_0 + \frac{1}{\rho_0 Re} \nabla_\eta^2 \hat{u}_1, \tag{26}$$

$$\frac{\partial \hat{p}_2}{\partial \tau'} + \rho_0 \nabla_\xi \hat{u}_1 = -\nabla_\eta \cdot (\hat{p}_2 \vec{u}_0), \tag{27}$$

$$\frac{\partial \hat{p}_{2a}}{\partial \tau'} + \gamma p_0 \nabla_\xi \hat{u}_1 = -\vec{u}_0 \cdot \nabla_\eta \hat{p}_{2a} - \gamma \hat{p}_{2a} \nabla_\eta \cdot \vec{u}_0 + \frac{\gamma}{RePr} \nabla_\eta^2 \hat{T}_2. \tag{28}$$

The equation of state at $O(\epsilon^2)$ is obtained as follows:

$$p_{2h} + p_{2a} = \rho_0 T_2 + \rho_2 T_0. \tag{29}$$

Equations (26)-(28) have derivatives with respect to two length scales (η and ξ). Assuming $u_0 \rightarrow 0$ as $\xi \rightarrow \infty$ (far away from the heat source), we derive governing equations for long wavelength acoustic waves as follows:

$$\frac{\partial \hat{u}_1}{\partial \tau'} + \frac{1}{\rho_0} \nabla_\xi \hat{p}_{2a} = \frac{1}{Re} \nabla_\eta^2 \hat{u}_1, \tag{30}$$

$$\frac{\partial \hat{p}_2}{\partial \tau'} + \rho_0 \nabla_\xi \hat{u}_1 = 0, \tag{31}$$

$$\frac{\partial \hat{p}_{2a}}{\partial \tau'} + \gamma p_0 \nabla_\xi \hat{u}_1 = \frac{\gamma}{RePr} \nabla_\eta^2 T_2. \tag{32}$$

From Eqs. (30)-(32), we see that long wavelength acoustic waves are subjected to dissipation. These dissipation terms are not found in the analysis of Wu *et al.*^{14,15} When dissipative forces cannot be neglected, such as low to moderate Reynolds number flows, our analysis gives a better description of the acoustic-hydrodynamic interaction. Equations (30)-(32) form a dissipative system, leading to the damping of the long wavelength acoustic waves.

Next, we introduce short length scale equations, by assuming a solution of the form $A(\eta, \tau') e^{i\omega\tau}$ for acoustic field variables,

$$\frac{\partial \hat{u}_1}{\partial \tau'} + \vec{u}_0 \cdot \nabla_\eta \hat{u}_1 + \hat{u}_1 \cdot \nabla_\eta \vec{u}_0 = -\frac{1}{\rho_0 Re} \nabla_\eta^2 \hat{u}_1, \tag{33}$$

$$\frac{\partial \hat{p}_2}{\partial \tau'} + \nabla_\eta \cdot (\hat{p}_2 \vec{u}_0) = 0, \tag{34}$$

$$\frac{\partial \hat{p}_{2a}}{\partial \tau'} + \vec{u}_0 \cdot \nabla_\eta \hat{p}_{2a} + \gamma \hat{p}_{2a} \nabla_\eta \cdot \vec{u}_0 = \frac{\gamma}{RePr} \nabla_\eta^2 \hat{T}_2. \tag{35}$$

Equations (33)-(35) describe the acoustic-hydrodynamic coupling equations. These equations resemble the wave-mean flow coupling mechanisms proposed by Buhler² for atmospheric flows. The wave and mean flow variables are chosen depending on the physical phenomena under investigation. As a result of our analysis of acoustic-hydrodynamic interaction, we obtain these variables as pressure and velocity corresponding to the acoustic and hydrodynamic fields. The terms $\hat{u}_1 \cdot \nabla_\eta \vec{u}_0$ and $\vec{u}_0 \cdot \nabla_\eta \hat{u}_1$ in Eq. (33) and the terms $\hat{p}_{2a} \nabla_\eta \cdot \vec{u}_0$ and $\vec{u}_0 \cdot \nabla_\eta \hat{p}_{2a}$ in Eq. (35) represent the mutual interaction of the wave and the mean flow.

The terms $\hat{u}_1 \cdot \nabla_\eta \vec{u}_0$ and $\vec{u}_0 \cdot \nabla_\eta \hat{u}_1$ represent the coupling between hydrodynamic and acoustic velocities. These terms are known as Reynolds forces in the study of nearly incompressible flows.²¹ These Reynolds forces, which describe the mutual transportation of the acoustic and hydrodynamic velocities, are also known as convective ($\vec{u}_0 \cdot \nabla_\eta \hat{u}_1$) and lift-up terms ($\hat{u}_1 \cdot \nabla_\eta \vec{u}_0$) in the study of transition to turbulence in fluid flow.²² Here, in a low Mach number reacting flow, convective and lift-up

mechanism could also establish a velocity coupling, where the acoustic velocity (\vec{u}_1) and the flow field (\vec{u}_0) in a combustor influence each other.

C. Nonlinear equations

For a reacting low Mach number flow, the dilatation term $\nabla_\eta \cdot \vec{u}_0$ in Eq. (35) is related to the heat release rate fluctuation. From Eq. (12),

$$\begin{aligned} \nabla_\eta \cdot \vec{u}_0 &= \frac{\gamma - 1}{\gamma p_0} HDa(\dot{Q} + \dot{Q}') \\ &+ \frac{\gamma - 1}{\gamma p_0 RePr} \nabla_\eta^2 T_0 - \frac{1}{\gamma p_0} \frac{\partial p_0}{\partial \tau'} \end{aligned} \quad (36)$$

The next step is to determine the influence of the heat release rate \dot{Q} and the fluctuation of heat release rate \dot{Q}' due to the acoustic field on the acoustic pressure field. Equation (36) for dilatation is substituted in Eq. (35) to obtain

$$\begin{aligned} \frac{\partial \hat{p}_{2a}}{\partial \tau'} + \vec{u}_0 \cdot \nabla_\eta \hat{p}_{2a} + \gamma \hat{p}_{2a} \left[\frac{\gamma - 1}{\gamma p_0} HDa(\dot{Q} + \dot{Q}') \right. \\ \left. + \frac{\gamma - 1}{\gamma p_0 RePr} \nabla_\eta^2 T_0 - \frac{1}{\gamma p_0} \frac{\partial p_0}{\partial \tau'} \right] &= \frac{\gamma}{RePr} \nabla_\eta^2 \hat{T}_2 \end{aligned} \quad (37)$$

Assuming an Arrhenius rate law and a single step chemical reaction, the heat release rate fluctuation \dot{Q}' due to the acoustic wave can be expressed as

$$\dot{Q}' = B \rho_2^2 XY e^{-E_a/RT}, \quad (38)$$

where B is the pre-exponential factor and the acoustic density perturbation ρ_2 is a function of τ and τ' . However, the heat release rate expansion ($\dot{Q} = \dot{Q}_0 + \dot{Q}'$) appears in Eq. (12) as well as in Eq. (37). To ensure the convergence of p_0 , we eliminate the fast time scale dependence of \dot{Q}' by expressing it in terms of $\hat{\rho}_2(\eta, t)$. Substituting the solution form $A_i(\eta, \tau') e^{i\omega\tau}$ in Eq. (29), we obtain

$$\hat{\rho}_2 = \frac{p_{2h}}{T_0} e^{-i\omega\tau} + \frac{\hat{p}_{2a}}{T_0} - \rho_0 \frac{\hat{T}_2}{T_0}. \quad (39)$$

As $\epsilon \rightarrow 0$, $\tau \rightarrow \infty$, because in the relation $\tau = \tau'/\epsilon$, we have assumed τ' of $O(1)$ and τ of $O(1/\epsilon)$. In the limit $\tau \rightarrow \infty$, $(p_{2h}/T_0) e^{-i\omega\tau} \rightarrow 0$. The expression for $\hat{\rho}_2$ can be rewritten as

$$\hat{\rho}_2 = \frac{\hat{p}_{2a}}{T_0} - \rho_0 \frac{\hat{T}_2}{T_0}. \quad (40)$$

The new expression for heat release rate fluctuation can be written as

$$\dot{Q}' = B \hat{\rho}_2^2 XY e^{-E_a/RT}. \quad (41)$$

First, the expression for $\hat{\rho}_2$ (i.e., Eq. (40)) is substituted in Eq. (41). Then, Eq. (41) becomes

$$\dot{Q}' = B \left(\frac{\hat{p}_{2a}^2 - 2\rho_0 \hat{p}_{2a} \hat{T}_2 + \rho_0^2 \hat{T}_2^2}{T_0^2} \right) XY e^{-E_a/RT}. \quad (42)$$

Equation (42) is then substituted in Eq. (37) to obtain

$$\begin{aligned} \frac{\partial \hat{p}_{2a}}{\partial \tau'} + \vec{u}_0 \cdot \nabla_\eta \hat{p}_{2a} &= \\ \frac{(\gamma - 1) HDa \omega}{p_0} \left(\frac{-\hat{p}_{2a}^3 + 2\rho_0 \hat{p}_{2a}^2 \hat{T}_2 - \rho_0^2 \hat{T}_2^2}{T_0^2} \right) &+ \\ + \frac{\gamma}{RePr} \nabla_\eta^2 \hat{T}_2 - \frac{(\gamma - 1) \hat{p}_{2a}}{p_0 RePr} \nabla_\eta^2 T_0 &- \\ - \frac{(\gamma - 1) HDa \omega \hat{p}_{2a}}{p_0} + \frac{p_{2a}}{p_0} \frac{\partial p_0}{\partial \tau'} \end{aligned} \quad (43)$$

where $\omega = BXYe^{-Ea/RT}$. Equation (43), which is a nonlinear equation, can be rewritten by grouping the terms of same order as

$$\begin{aligned} \frac{\partial \hat{p}_{2a}}{\partial \tau'} = & -\vec{u}_0 \cdot \nabla_{\eta} \hat{p}_{2a} + \alpha \hat{p}_{2a}^3 + \theta \hat{T}_2 \hat{p}_{2a}^2 \\ & + \vartheta \hat{T}_2^2 \hat{p}_{2a} + \lambda \hat{p}_{2a} + \frac{\gamma}{RePr} \nabla_{\eta}^2 \hat{T}_2. \end{aligned} \quad (44)$$

Substituting (40) in Eq. (34), we obtain an equation for T_2 ,

$$\begin{aligned} \frac{\partial \hat{T}_2}{\partial \tau'} = & -\vec{u}_0 \cdot \nabla_{\eta} \hat{T}_2 + \alpha \hat{T}_2 \hat{p}_{2a}^2 + \theta \hat{T}_2^2 \hat{p}_{2a} \\ & + \vartheta \hat{T}_2^3 + \lambda \hat{T}_2 + \frac{\gamma}{\rho_0 RePr} \nabla_{\eta}^2 \hat{T}_2. \end{aligned} \quad (45)$$

Equations (44) and (45) are nonlinear equations for acoustic pressure and second order thermal fluctuations, with the coefficients α , θ , and ϑ corresponding to the physical processes in the system such as heat release rate, temperature diffusion, pressure or temperature coupling, and the rate of change of the mean pressure p_0 . These nonlinear equations show that the amplitude of the acoustic pressure is coupled with the thermal fluctuation through volume expansion. Nonlinear equations Eqs. (44) and (45) represent this ‘‘pressure-temperature’’ coupling. Without the convection term ($u_0 \cdot \nabla_{\eta} p_{2a}$), the nonlinear equations resemble the RD systems discussed in the study of chemical oscillations,²³ where the effect of a nonlinear source term along with the diffusion term governs the stability of chemical reactions. Conventionally, the nonlinear term in the RD system is called a reaction term owing to its popular use in the study of the stability of chemically reacting systems. In a thermo-acoustic system, the stability is decided by the influence of fluid flow on the nonlinear nature of heat release rate-acoustic interaction. Theoretically, such an influence is understood by the incorporation of a convection term into the nonlinear equations. The convection term is present in our nonlinear equations. Therefore, the derived nonlinear equations are called CRD equations.

III. INSTABILITY MECHANISM

In the case of pressure coupling mechanism, the heat release rate fluctuation \hat{Q}' and acoustic pressure fluctuation \hat{p}_{2a} are of the same order.¹⁰ This is emphasized in Eq. (37), where \hat{Q}' and \hat{p}_{2a} appear at the same order ($O(\epsilon^2)$). In addition to the heat release rate fluctuation, convective terms are also present due to the acoustic-hydrodynamic interaction. Equation (44) derived from (37), thus, serves to explain the pressure coupling mechanism associated with the acoustic-hydrodynamic interaction. From Eqs. (44) and (45), we see that acoustic pressure is coupled with the thermal fluctuations due to interaction between acoustic field and heat release rate fluctuation. These equations together form a set of convection reaction diffusion equation.

A. Convection reaction diffusion equations

Equations (44) and (45) for acoustic pressure and thermal fluctuations are re-cast as follows:

$$\frac{\partial \hat{p}_{2a}}{\partial \tau'} + \vec{u}_0 \cdot \nabla_{\eta} \hat{p}_{2a} = f(\hat{p}_{2a}, \hat{T}_2) + \frac{\gamma}{RePr} \nabla_{\eta}^2 \hat{T}_2, \quad (46)$$

$$\frac{\partial \hat{T}_2}{\partial \tau'} + \vec{u}_0 \cdot \nabla_{\eta} \hat{T}_2 = g(\hat{p}_{2a}, \hat{T}_2) + \frac{\gamma}{\rho_0 RePr} \nabla_{\eta}^2 \hat{T}_2, \quad (47)$$

where $f(\hat{p}_{2a}, \hat{T}_2) = \alpha \hat{p}_{2a}^3 + \theta \hat{T}_2 \hat{p}_{2a}^2 + \vartheta \hat{T}_2^2 \hat{p}_{2a} + \lambda \hat{p}_{2a}$ and $g(\hat{p}_{2a}, \hat{T}_2) = \alpha \hat{T}_2 \hat{p}_{2a}^2 + \theta \hat{T}_2^2 \hat{p}_{2a} + \vartheta \hat{T}_2^3 + \lambda \hat{T}_2$ are nonlinear functions in the CRD equations. The coefficients in the nonlinear functions f and g are

$$\begin{aligned}
 \alpha &= -\frac{(\gamma - 1)HD_a\omega}{p_0T_0^2}, \\
 \theta &= 2\frac{(\gamma - 1)HD_a\omega}{p_0T_0^2}\rho_0, \\
 \vartheta &= -\frac{(\gamma - 1)HD_a\omega}{p_0}\rho_0^2, \\
 \lambda &= -\frac{(\gamma - 1)}{p_0RePr}\nabla_\eta^2T_0 - \frac{(\gamma - 1)HD_a\omega}{p_0} + \frac{1}{p_0}\frac{\partial p_0}{\partial \tau'}.
 \end{aligned} \tag{48}$$

These coefficients represent the important physical processes in a thermo-acoustic system. α , θ , and ϑ have the physical parameters governing the chemical reaction, i.e., the Damkohler number (D_a) and the reaction rate (ω). In combustors, these parameters are determined by the type of the fuel and the mass flow rate of fuel and air into the combustor. From Eqs. (40) and (41), we know that the nonlinear functions f and g represent the heat release rate fluctuation. The coefficients α , θ , and ϑ , therefore, are “weights” that determine the intensity of heat release rate fluctuation. The coefficient λ combines the effect of DC shift ($\frac{\partial p_0}{\partial \tau'}$), thermal diffusion ($\nabla_\eta^2T_0$), and the mean heat release rate ($HD_a\omega$). Since λ is the coefficient of the linear term, we see that the phenomena such as DC shift, thermal diffusion, and mean heat release rate contribute only to the linear growth of acoustic pressure amplitude. The change in mean pressure, known as “DC shift,” is a consequence of the heat release rate fluctuation due to the acoustic field as shown by Eq. (12). The close correlation of DC shift with the acoustic pressure oscillations was theoretically explained by Flandro *et al.*²⁴ They observed that, with the growth in mean pressure, there is an associated growth of the acoustic pressure amplitude. They proposed that the acoustic pressure could be a source term in the energy equation. This finding enabled them to design an algorithm that could help designing the rocket motors with reduced possibility of instability. Here, we have shown another mechanism-coupling of acoustic pressure oscillation with heat release rate fluctuation, as the cause for the change in mean pressure, and growth or decay of acoustic pressure oscillations. The heat release rate fluctuation in turn becomes a source term for DC shift. The representation of a thermo-acoustic system as a convective reaction diffusion system gives more insight into the stability characteristics. Many of the stability properties of a CRD system resemble that of a thermo-acoustic system.

B. An example demonstrating the transition to instability

In this section, we attempt to show the growth of a local perturbation to acoustic pressure, which eventually modifies the acoustic field. Such a modified acoustic field, with higher acoustic pressure amplitude may result due to the presence of a premixed flame in a duct^{14,15} or a localized heat release rate fluctuation.⁵ This process of growth in the acoustic pressure amplitude results from a small but finite amplitude initial perturbation to the acoustic field. Such a model problem, even though do not resemble closely a real combustor, serves the purpose of studying the nonlinear thermal-acoustic coupling found in a flame-acoustic interaction.

The model problem resembles a horizontal Rijke tube, with locally a higher heat release rate that arises from a local heat source. This higher heat release rate can arise from the local or nonuniform burning of vortices in a combustor.⁵ Everywhere else, we assume uniform heat release rate. We attempt to address the influence of localized higher heat release rate on the acoustic pressure amplitude. Such a localized heat release rate fluctuation is numerically implemented here with the weights of the nonlinear terms. We have given, locally, higher values for these weights (note that their value is proportional to the heat release rate) representing higher heat release rate. For example, in the present numerical configuration, at the location of the heat release rate fluctuation, we chose the values of α , θ , and ϑ to be 1.2 times their magnitude in other parts of duct, where the heat release rate is uniform. The species mass fractions are absorbed into the weights, as the mass fractions result in the heat release rate. Therefore, instead of separately prescribing the values of mass fractions, we prescribe the values of α , θ , and ϑ . Such an approach is made to reduce the

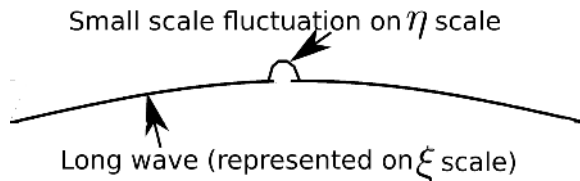


FIG. 1. Schematic of a small but finite amplitude local perturbation given to long scale acoustic field.

complexity of our mathematical model (i.e., CRD equations) and emphasize more on the nonlinear nature of instability.

The flame-acoustic interaction is governed by CRD equations written with respect to the short space scale variable. These equations also represent the evolution of initial perturbation to acoustic pressure field. The long space scale equations for acoustic field (Eqs. (30)-(32)) are not solved here. This is another advantage of the using MMS. The acoustic pressure amplitude $\hat{p}_{2a}(\eta, t)$ is separated from the acoustic pressure field $p_{2a}(\xi, t)$. The schematic representation of this separation is shown in Fig. 1. The numerical simulation of the convection reaction diffusion system (Eqs. (46) and (47)) is attempted here on a one dimensional domain representing a tube. 1D domain is represented by a spatial coordinate “x.” The discretization of 1D domain is done with different numbers of grid points ($N = 28, 56, 112, 224$). A grid convergence study shows that, for grid number $N = 56$ and above, solution remains the same. We have chosen $N = 56$ for the present numerical simulation. We impose a small but finite amplitude perturbation. To represent such a small perturbation, we use an initial condition shown in Fig. 3. CRD equations are for short space scale η . Long wavelength acoustic wave equations (30)-(32) are separate from the short space scale equations. The acoustic boundary conditions need to be applied only to the long space scale equations whose length scale is comparable to the tube length. The study of short scale fluctuations can be performed only when the localized sources are far away from the end points. For an open-open duct, boundary conditions (BC) at both end points is the same. This is a simple boundary condition to prevent spurious numerical oscillations. Also, we believe that this boundary condition is sufficient to study the growth of acoustic pressure amplitude due to the heat source. Here, the value of p_{2a} at the end point is extrapolated with the adjacent point (i.e., p_{2a} at $N = 56$ is equal to p_{2a} at $N = 55$. Similarly, p_{2a} at $N = 0$ is equal to p_{2a} at $N = 1$). The 1D geometry is shown in Fig. 2. The above discussed numerical configuration represents the model problem. The initial acoustic pressure perturbation is given in the middle of the 1D grid. The grid number is chosen to be $N = 56$. The initial condition for the acoustic pressure amplitude perturbation is shown in Fig. 3.

Here, the linear coefficient λ is chosen as the bifurcation parameter. Our choice is inspired by the efforts of Flandro *et al.*,²⁴ in determining the stability limits based on the DC shift. Apart from the DC shift, we also have heat release rate and thermal diffusion terms grouped inside λ .

Next, we use continuation algorithms employed in AUTO to study the bifurcations exhibited by CRD system. We observed two different types of bifurcations when the convection term is included in the computation of acoustic pressure amplitude. One type is a supercritical bifurcation with a secondary bifurcation and other type of bifurcation exhibits a hysteresis zone. Both types of bifurcations involve a bistable zone. A supercritical bifurcation, conventionally, is not known to cause bistability. However, when there is a secondary bifurcation, multiple stable branches may exist.²⁵

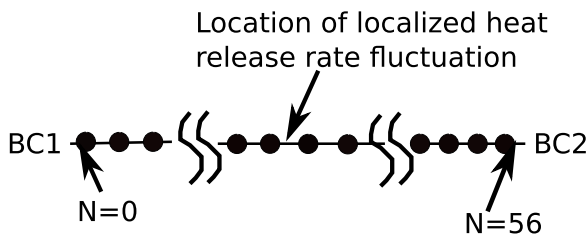


FIG. 2. 1D representation of an open-open tube with flame located in the centre.

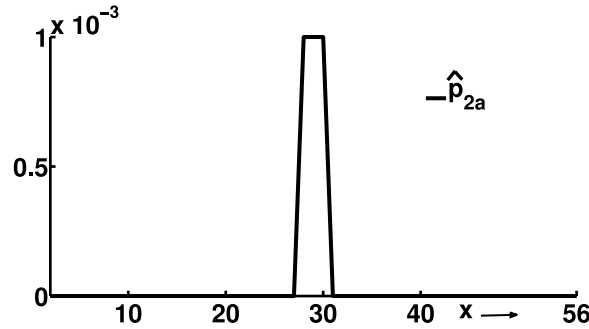


FIG. 3. The initial condition for acoustic pressure perturbation amplitude. X-axis shows the number of grid points representing the discretized 1D geometry.

The existence of bistable zone, resulting from a model nonlinear convection reaction diffusion equation, was discovered earlier in the study of the hydrodynamic stability by Chomaz.²⁶ He used a Ginzburg Landau model to study the influence of convection of the bifurcations observed in fluid flow instabilities. In the present study, we also point out the influence of nonlinear terms in (1) determining the saturation amplitude and (2) the threshold point (λ_h) at which the bifurcation occurs. Figures 4-6 show these nonlinear effects. We demonstrate these effects by varying the “weights” (θ and ϑ) of nonlinear terms.

For the values of ϑ of $O(10^{-2})$, CRD system permits the type of bifurcation shown in Fig. 4. Here, there exists a hysteresis region near the critical point λ_h . Such a hysteresis effect is widely studied in thermo-acoustics.^{27,28} In the previous investigations, transitions are described by a change from non-oscillatory to oscillatory state due to Hopf bifurcation. Here, we show the pitchfork bifurcation of the acoustic pressure amplitude. This is a consequence of separating the slow varying amplitude from oscillating solution on fast time scale. Here, a nonzero amplitude (\hat{p}_{2a}) represents an oscillatory solution ($p_{2a} = \hat{p}_{2a}e^{-i\omega\tau}$). In the vicinity of such a bifurcation, only a sufficiently large perturbation will lead to an oscillatory state. This process of introducing a large perturbation is called “triggering.” The significance of nonlinear terms in determining the saturation amplitude is discussed by Zinn and Lieuwen.²⁸ We have shown, while deriving nonlinear equations (46) and (47), that the nonlinear effects are introduced by the heat release rate fluctuations. Exploring the significance of the coefficients of nonlinear terms is therefore worthwhile. Next, we will explore the significance of the coefficients of other nonlinear terms.

The significance of θ is explained with the help of Fig. 5. The curve b1 in Fig. 5 is computed with $\theta = 0.6$, while λ is varied. The value of θ , used for the computation of b2 (i.e., $\theta = 0.9$) is greater than that used for the computation of b1, which implies the increase in saturation amplitude when θ is increased. Larger values of θ also increase the hysteresis width, by shifting λ_h away from the fold point at $\lambda = 0$ (λ_{h1} (for $\theta = 2$) $>$ λ_{h2} (for $\theta = 0.9$) $>$ λ_{h3} (for $\theta = 0.6$)). Therefore,

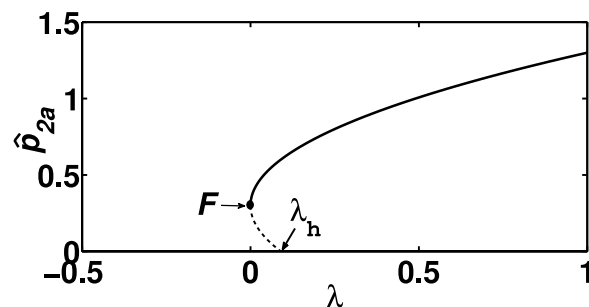


FIG. 4. Bifurcation for acoustic pressure amplitude p_{2a} . Dotted lines show unstable solutions. Solid lines indicate stable solutions. This type of bifurcation creates a hysteresis. The hysteresis zone exists in the control parameter range between F and $\lambda = \lambda_h$. Parameters chosen for the computation of this bifurcation diagram are $\alpha = -1$, $\theta = 0.6$, $\vartheta = 0.09$, and $u_0 = 1$.

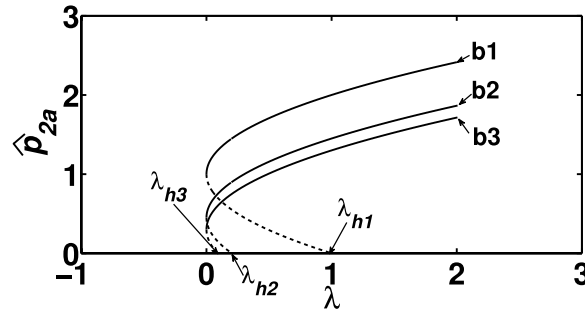


FIG. 5. Bifurcations of acoustic pressure amplitude computed with different values of θ and ϑ . Curve b1 is computed using the values $\theta=2$ and $\vartheta=-1$. Curve b2 is computed with $\theta=0.9$ and $\vartheta=-0.2025$. Curve b3 is computed with $\theta=0.6$ and $\vartheta=-0.09$. λ_{h1} , λ_{h2} , and λ_{h3} represent the critical values of λ at which bifurcation occurs for curves b1, b2, and b3, respectively.

from Fig. 5, we know that the role of θ is twofold: (1) first, the magnitude of θ determines the saturation amplitude and (2) then the value of θ determines the value of the control parameter at which bifurcation occurs. Here, larger values of θ imply that the magnitude of θ relative to the magnitude of ϑ is high. In real combustors, due to the intense heat, the mean density drops. Then, the magnitude of θ ($\propto \rho_0$) is greater than ϑ ($\propto \rho_0^2$). The physical insight from these computations is helpful in delaying or preventing the onset of instability. First, when there is an increase in θ , the triggering amplitude to reach the stable oscillatory solution is higher than the one that is needed for lower θ . Further, the onset of instability is delayed as a consequence of the shift in λ_h .

The change in hysteresis width in response to the variation in system parameters is an active area of investigation in thermo-acoustics. The reduction in hysteresis width with the decrease in mass flow rate is observed by various researchers^{29–31} for a Rijke tube. Gopalakrishnan and Sujith³¹ show that the variation in hysteresis width is related to the ratio of convective time scale to the acoustic time scale. In the present study, the “weights” of the nonlinear terms are functions of Damkohler number Da (ratio of flow time scale to the chemical time scale). Therefore, these weights definitely bear a relation to the mass flow rate in a combustor. A theoretical study performed by McIntosh³² claims that the burning rate is dependent on the acoustic time scale. A conjecture suggesting a relation between the chemical time scale and the acoustic time scale can be made. An investigation in this direction is promising, as it will establish a relation between instabilities in Rijke tube and the general thermo-acoustic instabilities.

Figure 6 shows the secondary bifurcation where, in spite of a supercritical bifurcation at $\lambda = \lambda_h$, there is a secondary fold bifurcation at F_1 (note that the value of ϑ is 0.01, which is relatively smaller than that used in the computation of Fig. 4). Further, we impose locally (at the

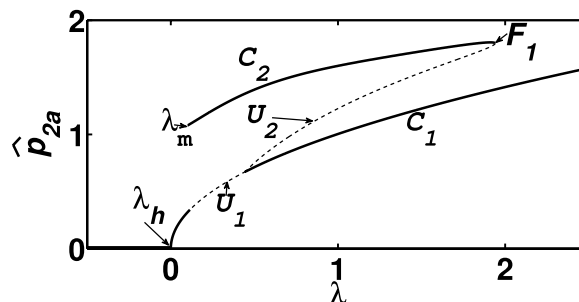


FIG. 6. Supercritical bifurcation exhibited by the acoustic pressure amplitude \hat{p}_{2a} . Dotted lines show unstable solutions. Solid lines indicate stable solutions. Further, a fold point bifurcation, indicated by F_1 creates a bistable zone. Parameters used for the computation are $\alpha=-1$, $\theta=1$, $\vartheta=0.01$, and $u_0=1$. F_1 denotes the fold point and bifurcation occurs at $\lambda = \lambda_h$. For $\lambda > \lambda_h$, system is absolutely unstable. For the convection reaction diffusion system, such a secondary bifurcation is obtained for any value of $\vartheta \leq 0.01$.

location of initial perturbation shown in Fig. 3) the values of α , θ , and ϑ to be 2 times their magnitude in other parts of duct. This implies a higher heat release rate than the one imposed in the numerical configuration discussed above. The fold bifurcation results in the creation of a second stable branch C_2 . The stable branch C_2 can be approached by the system in two ways: (1) by introducing any small perturbation, while system is in the parameter space corresponding to the unstable branch U_1 or (2) by introducing a sufficiently large amplitude perturbation (perturbation amplitude greater than the one corresponding to the unstable branch U_2), while system stays in the stable branch C_1 . When the second stable branch is attained, the system continues to stay in that branch till $\lambda = \lambda_m$. This can cause a hysteresis effect, widely studied in the field of thermoacoustic oscillations.

The magnitude of the coefficients of nonlinear terms is significant in determining the nature of bifurcation. These coefficients determine the intensity of heat release rate fluctuation. Therefore, by varying the magnitude of the coefficients, we vary the intensity of heat release rate fluctuation. We show that the variation in the intensity changes the nature of transition in a thermo-acoustic system.

The possibility of secondary bifurcation, creating a family of limit cycles in vibrating mechanical systems, was pointed out earlier by Ananthkrishnan *et al.*²⁵ They used a van der Pol oscillator model for the demonstration of secondary bifurcation. Later, Ananthkrishnan *et al.*³³ extended this reduced order model to show the existence of multiple limit cycle oscillations in thermo-acoustic systems. The existence of two stable oscillatory solutions for the same heat release rate parameter is obtained by Juniper.³⁴ He obtained these multiple stable states as the solutions of nonlinear momentum and energy equations. The nonlinear heat release rate term acts as a source to the energy equation. Juniper proposes the heat release rate to be dependent on the mean flow velocity ($\tilde{Q} \propto (u_0/3)^{1/2}$). The acoustic-mean flow interaction is therefore expected to cause multiple oscillatory state. The chemical reaction systems such as continuous stirred-tank reactor (CSTR) are also found to be exhibiting multiple oscillatory states.³⁵ The possibility of existence of a secondary bifurcation in our CRD system is explored in this paper.

For the configuration shown in Fig. 2, we attempt to study the change in the state of acoustic pressure while the strength of heat release rate caused by the flame is varied. In a real combustor, this variation can be implemented by the variation of the inflow of species and oxidizer (i.e., heat release rate is determined by the fuel-air mass fraction). The secondary bifurcation shown in Fig. 6 is obtained for low values of ϑ ($O(10^{-3})$). ϑ is one of the coefficients present in the nonlinear functions f and g . The presence of ρ_0^2 in ϑ and θ makes the nonlinear functions f and g dependent on the mean density in the combustor. The nonlinear functions govern the saturation amplitude of acoustic pressure. Therefore, the value of mean density has an influence on the bifurcation characteristics of thermo-acoustic system. The gas temperature variation that arises from the combustion results in the variation of density. Here, the mean density appears in the coefficients θ and ϑ . Therefore, the value of mean density decides the weight of the nonlinear terms. Various types of fluid dynamic instability arise in the reacting flows as a result of the variation in the density of gas.³⁶ Here, through the variation in the magnitude of ϑ and θ , we show that the density has a significant influence on the nature of bifurcation for acoustic pressure amplitude.

IV. CONCLUSION

We find that thermo-acoustic system has similarities with many wave-mean flow interacting systems. This viewpoint has helped us in developing a new theory for the transition to instability in a thermo-acoustic system. Considering the presence of two time scales in a wave-mean flow interaction system, we have employed MMS to understand thermo-acoustic interactions. Using MMS, two fundamental mechanisms of coupling, pressure-temperature coupling and velocity coupling, are derived from the compressible fluid flow equations. The pressure-temperature coupling is expressed through coupled convection reaction diffusion system of equations. The nonlinear terms represent the influence of heat release rate fluctuations. The separation of long scale wave equation from the short scale perturbation equations allows us to study the effect of short perturbations introduced by localized flames. These perturbation equations are proposed as a system of CRD equations. The

CRD equations are nonlinear and therefore predict the saturation amplitude. Therefore, the CRD system (Eqs. (44) and (45)) gives a better mathematical description of the nonlinear behavior of thermo-acoustic system in a low Mach number flow.

We observe two types of transitions: (1) through a bifurcation that causes a hysteresis region (shown in Fig. 4) and (2) through a secondary bifurcation (shown in Fig. 6). The secondary bifurcation was predicted in vibratory mechanical systems. In thermo-acoustics, the existence of multiple limit cycle can be observed experimentally. Theoretically, their existence was indicated using reduced order models (using van der Pol equations to model thermo-acoustic system). In this paper, derivation of a theoretical framework from the full compressible fluid flow equations, to predict multiple limit cycle, is attempted for the first time. The significance of the coefficients of nonlinear terms in delaying the onset of bifurcation is an interesting outcome of our study. This phenomenon also implies the significance of heat release rate fluctuation in the transition to instability.

The representation of the velocity coupling through a convective and lift-up mechanism (Eq. (33)) is introduced for the first time. The significance of physical parameters such as heat release rate in determining the growth or decay of oscillations is emphasized. Finally, we can also infer, from the convection reaction diffusion equations, that the convective time scale governs the acoustic-hydrodynamic interaction. The coupling mechanisms discussed in this paper are inherent to flame-acoustic interactions in combustion chambers. The study of this interaction, influenced by the flow field, is an immediate application of our theoretical framework.

- ¹ G. P. Zank and W. H. Matthaeus, "Nearly incompressible hydrodynamics and heat conduction," *Phys. Rev. Lett.* **64**, 1243–1246 (1990).
- ² O. Bühler, *Waves and Mean Flows* (Cambridge University Press, 2009).
- ³ P. Hunana, G. P. Zank, and S. Dastgeer, "Nearly incompressible fluids: Hydrodynamics and large scale inhomogeneity," *Phys. Rev. E* **74**, 026302 (2006).
- ⁴ S. Dastgeer and G. P. Zank, "The transition to incompressibility from compressible magnetohydrodynamic turbulence," *Astrophys. J., Lett.* **640**, L195 (2006).
- ⁵ T. J. Poinso, A. C. Trouve, D. P. Veynante, S. M. Candel, and E. J. Esposito, "Vortex-driven acoustically coupled combustion instabilities," *J. Fluid Mech.* **177**, 265–292 (1987).
- ⁶ F. E. C. Culick, "Unsteady motions in combustion chambers for propulsion systems," Technical Report RTO-AG-AVT-039 AC/323(AVT-039)TP/103, RTO AGARDograph, 2006.
- ⁷ B. T. Zinn, "A theoretical study of nonlinear combustion instability in liquid-propellant rocket engines," *AIAA J.* **6**, 1966–1972 (1968).
- ⁸ G. Searby, "Acoustic instability in premixed flames," *Combust. Sci. Technol.* **81**, 221–231 (1992).
- ⁹ R. A. Dunlap, "Resonance of a flame in a parallel walled combustion chamber," Technical Report Project MX833, Aeronautical Research Center, University of Michigan, 1950.
- ¹⁰ P. Clavin, P. Pelce, and L. He, "One-dimensional vibratory instability of planar flames propagating in tubes," *J. Fluid Mech.* **216**, 299–322 (1990).
- ¹¹ P. Clavin, J. S. Kim, and F. A. Williams, "Turbulence-induced noise effects on high-frequency combustion instabilities," *Combust. Sci. Technol.* **96**, 61–84 (1994).
- ¹² P. Pelce and D. Rochwerger, "Vibratory instability of cellular flames propagating in tubes," *J. Fluid Mech.* **239**, 293–307 (1992).
- ¹³ G. H. Markstein, *Non-Steady Flame Propagation* (Pergamon, 1964).
- ¹⁴ X. Wu, M. Wang, P. Moin, and N. Peters, "Combustion instability due to the nonlinear interaction between sound and flame," *J. Fluid Mech.* **497**, 23–53 (2003).
- ¹⁵ X. Wu, "Asymptotic approach to combustion instability," *Philos. Trans. R. Soc., A* **363**, 1247–1259 (2005).
- ¹⁶ M. Matalon and B. J. Matkowsky, "Flames as gasdynamic discontinuities," *J. Fluid Mech.* **124**, 239–259 (1982).
- ¹⁷ F. E. C. Culick, "Nonlinear behavior of acoustic waves in combustion chambers I," *Acta Astronaut.* **3**, 715–734 (1976).
- ¹⁸ F. E. C. Culick, "Nonlinear behavior of acoustic waves in combustion chambers II," *Acta Astronaut.* **3**, 735–757 (1976).
- ¹⁹ R. Klein, N. Botta, T. Schneider, C. D. Munz, S. Roller, A. Meister, L. Hoffmann, and T. Sonar, "Asymptotic adaptive methods for multi-scale problems in fluid mechanics," *J. Eng. Math.* **39**, 261–343 (2001).
- ²⁰ A. H. Nayfeh, *Perturbation Methods* (Wiley-VCH, 2008).
- ²¹ S. Dastgeer and G. P. Zank, "Nonlinear flows in nearly incompressible hydrodynamic fluids," *Phys. Rev. E* **69**, 066309 (2004).
- ²² O. Marquet, M. Lombardi, J. M. Chomaz, D. Sip, and L. Jacquin, "Direct and adjoint global modes of a recirculation bubble: Lift-up and convective non-normalities," *J. Fluid Mech.* **622**, 1–21 (2009).
- ²³ Y. Kuramoto, *Chemical Oscillations, Waves, and Turbulence* (Springer-Verlag, New York, 1984).
- ²⁴ G. A. Flandro, S. R. Fischbach, and J. Majdalani, "Nonlinear rocket motor stability prediction: Limit amplitude, triggering, and mean pressure shift," *Phys. Fluids* **19**, 094101-01–094101-16 (2007).
- ²⁵ N. Ananthkrishnan, K. Sudhakar, S. Sudershan, and A. Agarwal, "Application of secondary bifurcations to large amplitude limit cycles in mechanical systems," *J. Sound Vib.* **215**, 183–188 (1998).
- ²⁶ J. M. Chomaz, "Absolute and convective instabilities in nonlinear systems," *Phys. Rev. Lett.* **69**, 1931–1934 (1992).

- ²⁷ P. Subramanian, R. I. Sujith, and P. Wahi, "Subcritical bifurcation and bistability in thermoacoustic systems," *J. Fluid Mech.* **715**, 210–238 (2013).
- ²⁸ B. T. Zinn and T. C. Lieuwen, "Combustion instabilities: Basic concepts," in *Combustion Instabilities in Gas Turbine Engines: Operational Experience, Fundamental Mechanisms, and Modeling*, edited by T. C. Lieuwen and V. Yang (American Institute of Aeronautics and Astronautics, Reston, VA, 2006), Chap. 1, pp. 3–26.
- ²⁹ K. I. Matveev, "Thermoacoustic instabilities in the Rijke tube: Experiments and modeling," Ph.D. thesis, California Institute of Technology, 2003.
- ³⁰ S. Mariappan, "Theoretical and experimental investigation of the non-normal nature of thermoacoustic interactions," Ph.D. thesis, Indian Institute of Technology Madras, 2011.
- ³¹ E. A. Gopalakrishnan and R. I. Sujith, "Influence of system parameters on the hysteresis characteristics of a horizontal Rijke tube," *Int. J. Spray Combust. Dyn.* **6**, 293–316 (2014).
- ³² A. C. McIntosh, "Pressure disturbances of different length scales interacting with conventional flames," *Combust. Sci. Technol.* **75**, 287–309 (1991).
- ³³ N. Ananthkrishnan, D. Shardul, and F. E. C. Culick, "Reduced-order modeling and dynamics of nonlinear acoustic waves in a combustion chamber," *Combust. Sci. Technol.* **177**, 221–248 (2005).
- ³⁴ M. P. Juniper, "Triggering in the horizontal Rijke tube: Non-normality, transient growth and bypass transition," *J. Fluid Mech.* **667**, 272–308 (2011).
- ³⁵ P. Lamba and J. L. Hudson, "Experimental evidence of multiple oscillatory states in a continuous reactor," *Chem. Eng. Commun.* **32**, 369–375 (1985).
- ³⁶ B. Emerson, J. O'Connor, M. Juniper, and T. Lieuwen, "Density ratio effects on reacting bluff-body flow field characteristics," *J. Fluid Mech.* **706**, 219–250 (2012).